

Carbon Monoxide Adsorption on a $\text{Cu}_3\text{Pt}(111)$ Single Crystal Alloy

Y. G. Shen, D. J. O'Connor and R. J. MacDonald

Department of Physics, University of Newcastle,
Newcastle, NSW 2308, Australia.

Abstract

The adsorption of CO on $\text{Cu}_3\text{Pt}(111)$ was investigated by low energy He^+ ion scattering. The alloy surface was characterised by low energy electron diffraction (LEED) and work function change ($\Delta\phi$) measurements. No surface ordering of the alloy was evidenced by LEED. The CO induced work function changes were small. Under normal incidence of the beam, only the scattered He^+ ions from O, Cu and Pt were detected, indicating the orientation of the CO molecule with O facing away from the surface. In the initial stages of CO adsorption at 200 K, the Pt intensity in a Cu-rich surface was not detectable at an exposure of ~ 5 L CO, indicating that all the Pt atoms were covered by CO. At a saturation coverage of CO, the Pt intensity in a Pt-rich surface, however, fell to $\sim 12\%$ of its clean surface intensity. This observation strongly suggested that not all the Pt sites were covered by the CO molecules. These results are discussed in relation with the structure and composition of the surface and compared to data for CO adsorption on Pt(111).

1. Introduction

The physical and chemical properties of bimetallic alloy surfaces have been the subject of several theoretical and experimental studies in recent years. The Cu–Pt alloys are believed to be very interesting catalysts for hydrocarbon reactions and oxidation of CO to CO_2 (Jonstec and Ponec 1980). It is well known that the Cu–Pt alloy system forms a continuous substitutionally disordered structure at high temperatures, while at low temperatures three ordered phases (Cu_3Pt , CuPt and CuPt_3) are formed (Hansen and Anderko 1958). The alloys in the Cu_3Pt region with Pt less than about 24 at% have the L1_2 (Cu_3Au -type) structure in the whole temperature range below the critical ordering temperature T_c . It has also been reported (Mitsui *et al.* 1986), however, that the phase stability of the L1_2 structure with respect to L1_{2-s} (long period ordering structure) and A1 (disordered) phases is rather weak. The L1_{2-s} phase only occurs in a narrow temperature range near the stoichiometric composition.

For Cu–Pt alloys, surface segregation, chemisorption and catalytic activity have been investigated by various experimental spectroscopies and techniques (see e.g. Langeveld and Ponec 1983; Shek *et al.* 1983; Arola *et al.* 1991). Much of the existing experimental work on Cu–Pt has involved polycrystalline samples. A number of theoretical studies of the electronic structure of the Cu–Pt system have been reported in the literature (Banhart *et al.* 1989; Castro and Doyen 1994). Recently, adsorption behaviour of the (111) face of the Cu_3Pt crystal

has been studied by Castro *et al.* (1992) using thermal desorption spectroscopy (TDS), high-resolution electron energy loss spectroscopy (HREELS), ultraviolet photoelectron spectroscopy (UPS) and work function change ($\Delta\phi$) measurements. These investigations have shown that CO is molecularly bonded to the Pt site through the carbon atom. The structure of clean Cu₃Pt(111) has also been investigated recently by the present authors using low energy ion scattering (LEIS) with alkali ions and low energy electron diffraction (LEED) (Shen *et al.* 1995*a*). No surface chemical ordering or reconstruction has been evidenced. The surface disordering effect in this alloy has been confirmed very recently by scanning tunnelling microscopy (STM) measurements (Schröder 1995), revealing a direct image of the statistical distributions of the Pt atoms in the surface layer.

The two different surface composition phases (Cu-rich and Pt-rich) have been evidenced depending on sputtering and annealing conditions. The present work aims to reveal the possible different reactivities of the two kinds of surface Pt composition upon CO adsorption. We also tried to elucidate some features of the interaction of CO with Cu₃Pt(111). This study has been performed using low energy He⁺ ion scattering with a combination of LEED and $\Delta\phi$ measurements. Results of these measurements are compared and discussed with respect to those obtained on Pt(111). The use of noble gas He⁺ projectiles, which have extremely high rates of neutralisation during scattering events, ensures a high degree of surface sensitivity (see e.g. reviews by Niehus *et al.* 1993; Rabalais 1994).

2. Experimental

Our angle resolved ion scattering system, Colutron ion source and experimental methods have been described previously (Shen *et al.* 1995*b*, 1995*c*). Briefly, the UHV chamber ($\sim 1 \times 10^{-10}$ mbar base pressure) was equipped with a three-grid LEED system. A Kelvin probe has recently been installed for $\Delta\phi$ measurements. The angle of incidence α , measured from the sample surface plane, was calibrated to $\pm 0.5^\circ$ by aligning a He-Ne laser along the ion beam direction. The azimuthal angle ϕ was measured from the $[0\bar{1}1]$ and $[1\bar{2}1]$ azimuths of clean Cu₃Pt(111). The angle was initially determined by LEED measurements and then more finely adjusted using azimuthal scans in LEIS to give an estimated accuracy of $\leq 1^\circ$. The scattered ions were energy analysed by a hemispherical electrostatic analyser ($\Delta E/E = 0.02$), which is rotatable to allow total laboratory scattering angles θ from 0 to 130° with a resolution of 1° . The analyser was equipped with a dual multichannel plate detector (MCD) to provide high count rates. The use of MCD allows data collection with small ion doses, typically $< 1 \times 10^{13}$ ions/cm² per full energy spectrum at a beam current density of $\sim 2 \times 10^{-8}$ A/cm² for 1 keV He⁺ ions used in this study. As a measure of the peak (O, Pt and Cu) intensities, the integrated yields were used with linear background subtraction.

The well oriented ($\leq 0.5^\circ$) and polished Cu₃Pt(111) sample had been used and extensively cleaned in previous measurements (Shen *et al.* 1995*a*). The crystal surface was cleaned by Ar⁺ ion bombardment plus several heating/cooling cycles between 300 and 800 K in 1×10^{-7} mbar O₂. Final cleaning was achieved by heating to 850 K (below an order-disorder phase transition temperature of ~ 870 K for Cu₃Pt). The temperature was measured by means of a chromel-alumel thermocouple, directly spot welded to the edge of the sample. Surface cleanliness was verified by the absence of O, S and C in the He⁺ LEIS spectra.

The crystal could be cooled to 200 K. CO exposure measurements were carried out by back-filling the chamber with research purity CO through a leak valve to the desired pressure. All exposures are expressed in Langmuir units ($1 \text{ L} = 10^{-6} \text{ Torr.s} = 1.33 \times 10^{-4} \text{ Pa.s}$) based on uncorrected ion gauge readings. The CO coverage on the alloy surface has been obtained after calibration of the clearest $c(4 \times 2)$ LEED pattern with respect to the CO coverage on Pt(111) for $\theta_{\text{CO}} = 0.5 \text{ ML}$ ($\sim 10 \text{ L}$) at 200 K, where one monolayer corresponds to one CO per Pt surface atom. The adsorbed CO was totally removed by flashing the crystal to 550 K.

Depending on sputtering and annealing conditions the two different surface composition phases can be prepared: annealing at 850 K results in a slightly Cu-rich surface (20 at% Pt); sputtering followed by annealing at 500 K results in a Pt-rich surface (32 at% Pt). The saturation coverage measured in the LEIS experiments was approximately $\theta_{\text{CO}} = 0.22 \text{ ML}$ ($\sim 5 \text{ L}$) for a Cu-rich surface and $\theta_{\text{CO}} = 0.35 \text{ ML}$ ($\sim 8 \text{ L}$) for a Pt-rich surface, respectively. On a day to day basis, the two surface states were reproducible for surface preparation in the same way within the experimental uncertainty. Special care was taken to minimise sputtering-induced damage, roughening and selective removing of CO by the ion beam. No significant effect of ion induced desorption was observed during the measurement. Sputtering of the CO was experimentally measured to be less than 0.02 ML of its original coverage for the time required to collect each spectrum (10 s).

3. Results

(3a) Surface Characterisation

Both Cu-rich and Pt-rich $\text{Cu}_3\text{Pt}(111)$ surfaces showed a sharp LEED 1×1 pattern with low background corresponding to a unreconstructed surface without long range order of the Cu and Pt atoms. Neither (2×2) nor $(\sqrt{3} \times \sqrt{3}) R30^\circ$ ordered structure was observed. A total of about 200 h annealing at 800 K was found to be still not sufficient to develop a high degree of surface order. No superstructures were found following the adsorption of CO at 200 K. The (1×1) pattern remained clearly distinguishable during all CO experiments.

The surface composition measured by LEIS has been quantified in the following way (Shen *et al.* 1992): for a given binary alloy Cu–Pt, the surface composition of the Pt element in the alloy is given to first approximation by $c_{\text{Pt}} = I_{\text{Pt}} / (I_{\text{Pt}} + s_{\text{Pt/Cu}} I_{\text{Cu}})$, where I_{Pt} and I_{Cu} are the intensities of the ions scattered at Pt and Cu atoms, respectively, and $s_{\text{Pt/Cu}}$ denotes the relative sensitivity factor of Pt atoms to Cu atoms, which is also corrected by their atomic densities for pure elements. In the experiments reported here, the ratio $s_{\text{Pt/Cu}}$ was obtained by using standard measurements on pure Pt(111) and Cu(111) single crystals under identical experimental conditions. Evaluating the accuracy of the surface composition measured gives an uncertainty of about $\pm 2 \text{ at\%}$. This determination of surface composition using standard measurements on pure elements is limited to the clean alloy surface.

In order to test the annealing behaviour of the preferentially sputtered surface, the variation of the Pt component of the surface composition starting from the sputtered surface was recorded during both heating and cooling. Temperature

changes are believed not to affect the ion fraction. The result of such an experiment is shown in Fig. 1, where Pt composition in the first layer is plotted as a function of temperature along the $[\bar{1}\bar{2}1]$ azimuthal direction at an incident angle of $\alpha = 55^\circ$ and a scattering angle of $\theta = 110^\circ$. The results show that preferential sputtering causes Pt enrichment to a value of $\text{Cu}_{68}\text{Pt}_{32}$ in the surface layer. The Pt composition in the first layer is found to decrease only slightly with increasing temperature up to 600 K. This observation suggests that the surface composition equilibrium is not reached due to the low diffusion rate below 600 K. This also means that surface diffusion cannot lead to a direct exchange between first layer and second layer atoms in the $\text{Cu}_3\text{Pt}(111)$ surface. During further annealing in the temperature range 600 to 800 K, exchange of atoms between the first few layers becomes possible, and slight Cu enrichment in the first layer at equilibrium is observed. This result also indicates that the thermal equilibrium phase is finally reached above 800 K. Annealing at lower temperatures again (during cooling) does not change the surface composition any further.

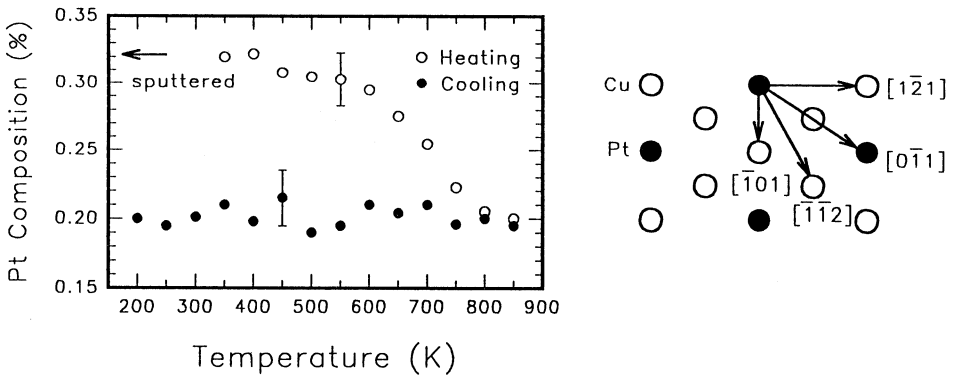


Fig. 1. Pt composition in the first layer as a function of alloy temperature measured with 1 keV He^+ ions at $\alpha = 55^\circ$ and $\theta = 110^\circ$ along the $[\bar{1}\bar{2}1]$ azimuth. From each point (\circ), data were taken during heating at 20 K min^{-1} , held for 5 min and then the energy spectrum was taken. The other data points were taken during cooling; the sample was held at 850 K for several minutes, cooled to the observation temperature and held for 5 min (\bullet). Before measurement, the alloy was sputtered with $>2 \times 10^{16} \text{ Ar}^+$ ions/ cm^2 ($E_0 = 2 \text{ keV}$). A schematic top view of the first layer atoms on an ordered $\text{Cu}_3\text{Pt}(111)$ surface is shown on the right-hand side.

(3b) Azimuthal Angle Scans from $\text{Cu}_3\text{Pt}(111)$, $\text{Pt}(111)$ and $\text{Cu}(111)$

The results of the azimuthal scan for Cu and Pt intensities from the two surface states of the $\text{Cu}_3\text{Pt}(111)$ crystal at grazing incidence are shown in Figs 2a and 2b respectively. The azimuthal scans from the clean $\text{Cu}(111)$ and $\text{Pt}(111)$ surfaces under identical scattering geometries are also shown in Figs 2c and 2d for comparison. The symmetry of the crystal structure can be obtained directly from the shadowing dips along the main crystallographic directions. These shadowing features contain information on the surface periodicity. Pronounced deep minima are observed at the azimuthal positions corresponding to alignment of the beam along specific directions. For the two surface states in $\text{Cu}_3\text{Pt}(111)$, these pronounced minima (Figs 2a and 2b) are a result of shadowing and blocking

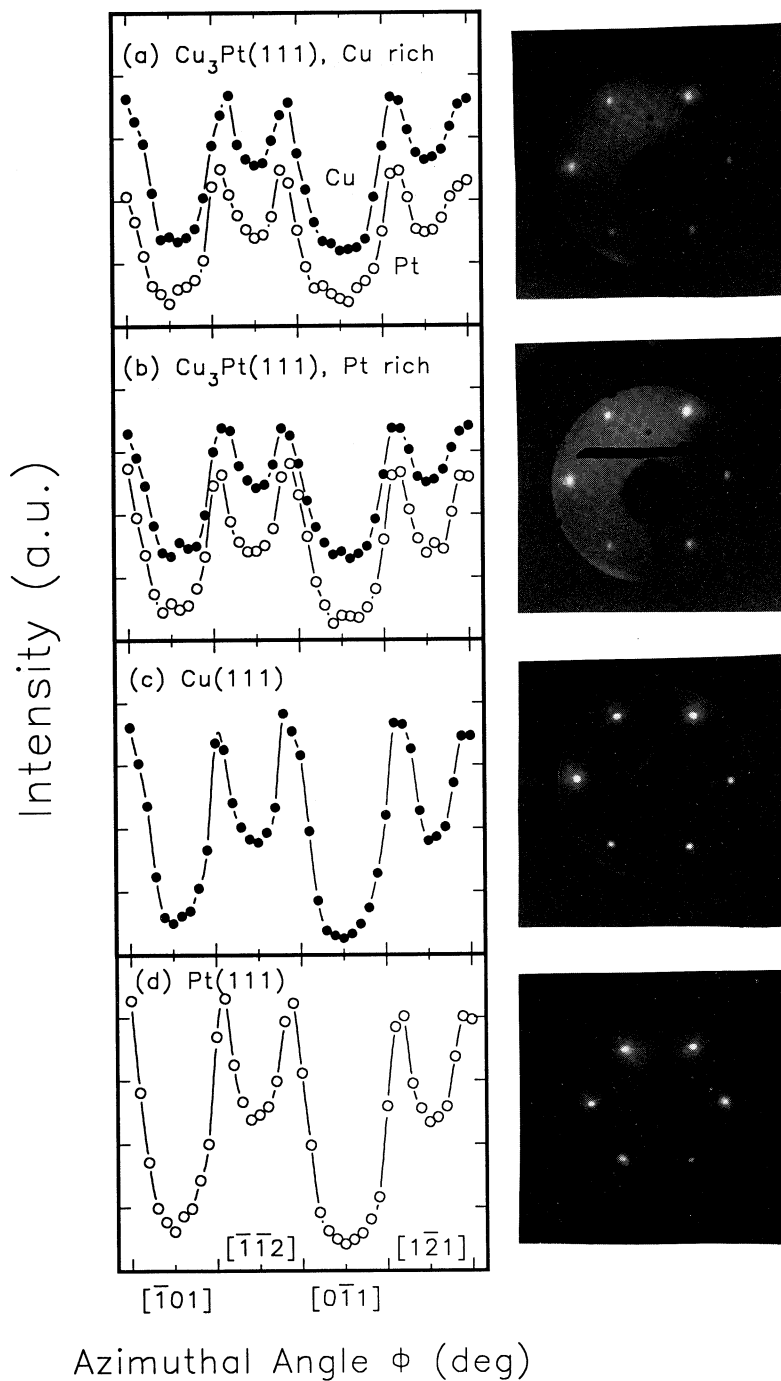


Fig. 2. Azimuthal distributions of 1 keV He^+ ions from (a) the Cu-rich and (b) the Pt-rich $\text{Cu}_3\text{Pt}(111)$ surfaces and (c) the $\text{Cu}(111)$ and (d) the $\text{Pt}(111)$ surfaces at grazing incidence of $\alpha = 8^\circ$ at a fixed scattering angle of $\theta = 110^\circ$. Photographs of LEED patterns for Cu-rich $\text{Cu}_3\text{Pt}(111)$ (64 eV), Pt-rich $\text{Cu}_3\text{Pt}(111)$ (64 eV), $\text{Cu}(111)$ (78 eV) and $\text{Pt}(111)$ (70 eV) are shown on the right-hand side.

along short azimuths $[\bar{1}01]$ and $[0\bar{1}1]$ (separated by 60°) where the interatomic spacing is 2.62 \AA . Less pronounced minima along long azimuths $[\bar{1}\bar{1}2]$ and $[\bar{1}\bar{2}1]$ (also separated by 60°) are observed where the interatomic distance is 4.52 \AA . This procedure guarantees that the alloy surface is clean and exhibits good short range order. The azimuthal data presented here cannot, however, determine the chemical ordering of the Cu-Pt surface, but the LEED patterns certainly suggest no long range order (without 2×2 ordered structure) on the crystal surface, as mentioned above (also see photographs of LEED patterns on the right-hand side of Fig. 2).

(3c) $\Delta\phi$ Measurements

Previous studies (Tüshaus *et al.* 1987; Schweizer *et al.* 1989) on CO/Pt(111) indicate that, at low coverages, the CO molecules bond only to the Pt sites of Pt(111). Population of the bridge-sites is observed for $\theta_{\text{CO}} > 0.33 \text{ ML}$. At $\theta_{\text{CO}} = 0.5 \text{ ML}$, a $c(4 \times 2)$ phase is formed in which half of the CO molecules are adsorbed on-top sites and the other half on-bridge sites (Tüshaus *et al.* 1987; Schweizer *et al.* 1989). Our measurements for changes in the $\Delta\phi$ values relative to CO adsorption on the Pt(111) and $\text{Cu}_3\text{Pt}(111)$ crystal surfaces at 200 K are shown in Fig. 3. For Pt(111), by using the calibration of θ_{CO} versus exposure as derived from LEED, it was found that the $\Delta\phi_{\text{min}}$ occurs at coverage around 0.33 ML ($\sim 6 \text{ L CO}$) and $\Delta\phi \approx 0.0 \text{ eV}$ at $\theta_{\text{CO}} = 0.5 \text{ ML}$ ($\sim 10 \text{ L CO}$). This is in agreement with the literature data (Norton *et al.* 1979; Steininger *et al.* 1982). For $\text{Cu}_3\text{Pt}(111)$, CO adsorption on both surface states provokes a work function increase by no more than $\sim 40 \text{ meV}$. These results agree with the $\Delta\phi$ values measured by Schneider *et al.* (1994), revealing that the chemisorbed CO induces almost no increase of the work function.

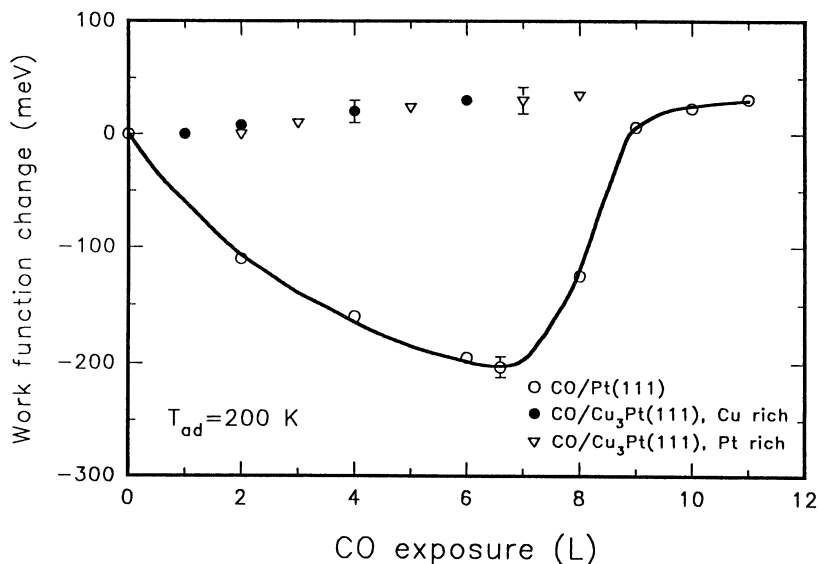


Fig. 3. Work function change $\Delta\phi$ of the Pt(111) and $\text{Cu}_3\text{Pt}(111)$ surfaces as a function of CO exposure at 200 K .

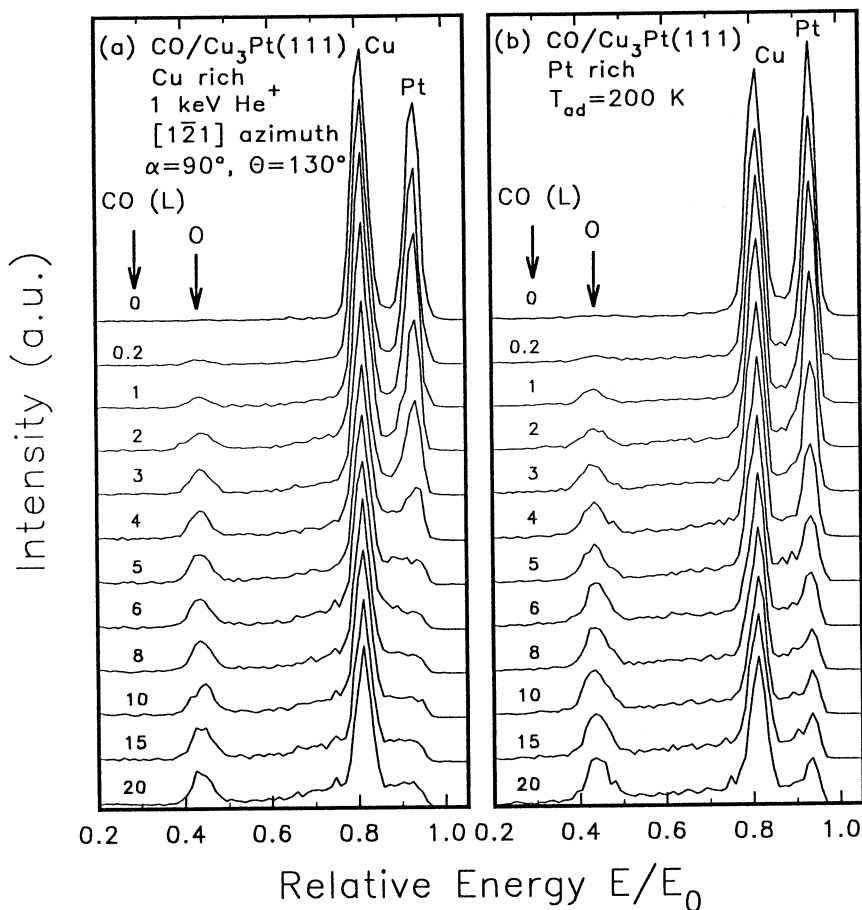


Fig. 4. Energy spectra for 1 keV He^+ ions scattered from clean and CO-exposed $\text{Cu}_3\text{Pt}(111)$. Exposures were carried out at a CO pressure of 5×10^{-8} mbar at 200 K. (a) the Cu-rich surface (well annealed) and (b) the Pt-rich surface (Ar bombardment followed by annealing at 500 K for a short time to remove the sputtering damage).

(3d) CO Adsorption by He^+ Ion Scattering

Before CO adsorption, the alloy surface was prepared by the two different methods and then cooled down to 200 K. Typical He^+ energy spectra taken from clean and CO-covered $\text{Cu}_3\text{Pt}(111)$ surfaces at different CO exposures are shown in Fig. 4. For comparison, the energy spectra collected from the Pt(111) and Cu(111) surfaces under identical experimental conditions are shown in Fig. 5. In these experiments the ion beam was at $\alpha = 90^\circ$ (normal incidence) along the $[1\bar{2}1]$ exit azimuth at $\theta = 130^\circ$. Under these conditions, the crystallographic surface effects are of minor importance. As CO is adsorbed, the O peak intensity increases while the Pt and Cu intensities decrease. All three peaks appear near the values of E/E_0 expected from the binary collision approximation model (see Niehus *et al.* 1993): 0.93 for Pt, 0.81 for Cu and 0.43 for O.

Since low energy He^+ ion scattering is extremely sensitive to the topmost surface layer, these observations lead to the conclusion that CO adsorbs in an

upright orientation of the molecule with O facing away from both the Pt(111) and Cu₃Pt(111) surfaces. An important feature of Fig. 4 is that the Pt intensity is no longer detectable at longer exposures in a Cu-rich surface (Fig. 4*a*) in contrast to the remaining presence of a small Pt peak intensity in a Pt-rich surface (Fig. 4*b*). The Pt intensity from the reference sample of Pt(111) in Fig. 5*a* decreases with increasing CO coverage. At a saturation coverage of CO, a considerable Pt peak intensity still remains. In Fig. 5*b*, the O signal is not detectable for CO adsorption on Cu(111). The fact that the Cu intensity remains unchanged before and after CO adsorption indicates that the CO does not adsorb on Cu(111) at this adsorption temperature. This is in agreement with the literature data (Persson 1992), which indicate that the CO adsorbs on Cu(111) only at low adsorption temperature (<180 K).

To further understand the effect of CO adsorption at low temperature under UHV conditions, a systematic study of CO adsorption on the two surface states was performed. Figs. 6*a* and 6*b* show the variation in the Pt and Cu intensities as a function of CO exposure for the Cu-rich and Pt-rich surfaces, respectively. Each Pt (Cu) datum point was normalised to that corresponding to the freshly cleaned Pt (Cu) signal intensity. Fig. 6*c* shows the results obtained from the CO/Pt(111) surface as reference. These figures also show the O intensity with the CO coverage in the insets. The Pt intensity for CO on Pt(111) (Fig. 6*c*) exhibits a linear decline by about 50% when the Pt(111) surface is partially covered by ~6 L CO. The Pt signal continues to decrease as the CO coverage increases, but with decreasing slope. At a CO exposure of ~10 L, the attenuation of the Pt intensity shows about 35% of the clean surface intensity. The ion scattering results suggest that a CO molecule can block more than one Pt atom. This can be ascribed to a combined effect of site blocking and neutralisation.

From the results in Figs 6*a* and 6*b*, the following two statements can be made: First, during the initial stages of CO adsorption the Pt intensity decreases much faster than the Cu intensity. This leads to the hypothesis that the chemisorptive CO is preferentially occupying on-top Pt sites. Second, the Pt intensity in a Cu-rich surface is not detectable after an exposure of ~5 L CO (Fig. 6*a*), indicating that all the Pt atoms are covered by CO. At a saturation coverage of CO, the Pt intensity in a Pt-rich surface, however, falls to ~12% of its clean surface intensity, as shown in Fig. 6*b*. This observation strongly suggests that not all of the Pt surface atoms are covered by the CO molecules in the Pt-rich Cu₃Pt(111) surface. Experiments along a random (high-index) direction under identical adsorption conditions (not shown) provided the same results as above.

During CO adsorption, the Cu signal is also suppressed. The Cu intensity falls to about 70% (60%) of its clean surface intensity for the Cu-rich (Pt-rich) surface. In separate two exposure experiments on Cu-rich and Pt-rich Cu₃Pt(111) surfaces under identical adsorption conditions (not shown), the ion beam was at normal incidence along the short [0 $\bar{1}$ 1] exit azimuth. The results indicate that the decrease in the Cu intensity and eventually falling to about 70% (60%) of its clean surface intensity is almost azimuthal independent within ± 10 –15%.

Possible reasons for the decrease in the Cu intensity upon CO adsorption can be: (a) the Cu sites are partially covered by CO; (b) the presence of the CO adsorbate layer on the alloy surface induces a surface segregation of Pt and disappearance of some Cu atoms from the first layer; and (c) changes in

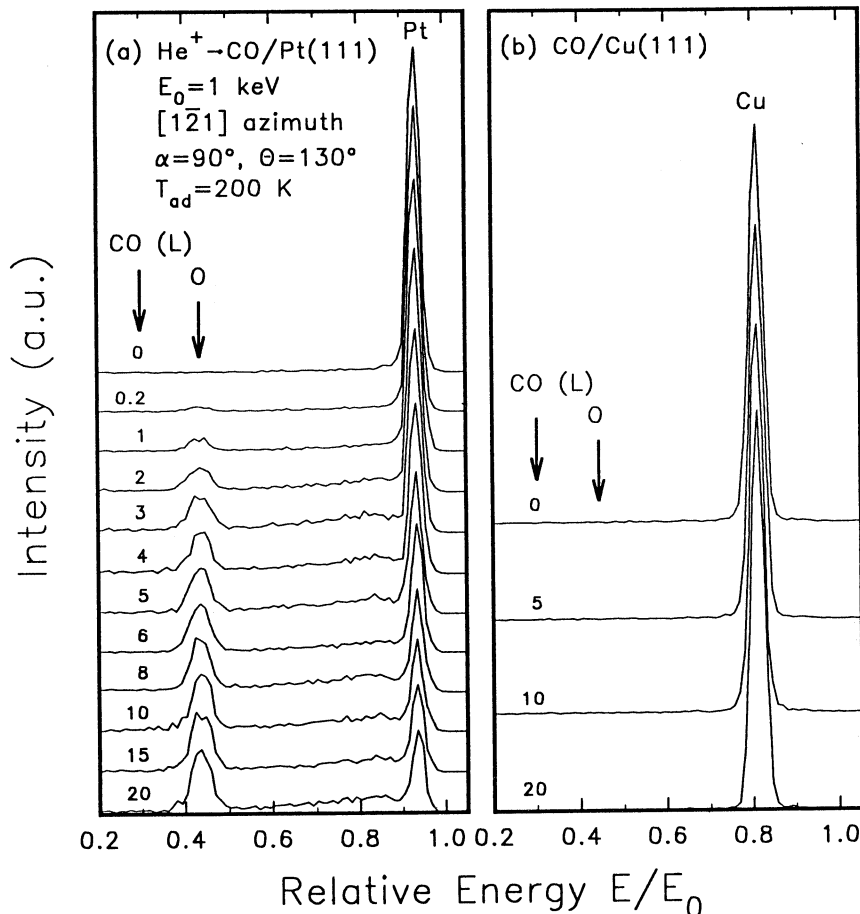


Fig. 5. Energy spectra for 1 keV He⁺ ions scattered from clean and CO-exposed (a) Pt(111) and (b) Cu(111). Exposures were carried out at a CO pressure of 5×10^{-8} mbar at 200 K.

neutralisation rate due to localisation of electrons in the CO-bound surface. The suggestion that the Cu sites are partially covered by CO in the initial stages of CO adsorption is very unlikely since our measurement on the CO/Cu(111) system shows that CO does not adsorb on Cu(111) at this temperature (Fig. 5b). It has also been reported (Castro *et al.* 1992; Schneider *et al.* 1993) that CO does adsorb on the Cu sites in the Cu₃Pt(111) surface only at a very low adsorption temperature (~ 50 K). It might be possible that the CO adsorption induces segregation of the Pt atoms from the bulk and exchange of some Cu atoms in the first layer. To exclude this possibility we have compared the Pt signals measured from the Cu₃Pt(111) surface before CO adsorption and after CO desorption. The Pt intensity obtained from both cases is the same within the experimental uncertainty, so the surface segregation of Pt induced by CO chemisorption cannot be the reason for the decrease of the Cu intensity. Based on Hagstrum's (1954) model, the main neutralisation mechanism for noble gas ion scattering is an Auger process. An electron tunnels from the Cu (3d)-Pt (5d)

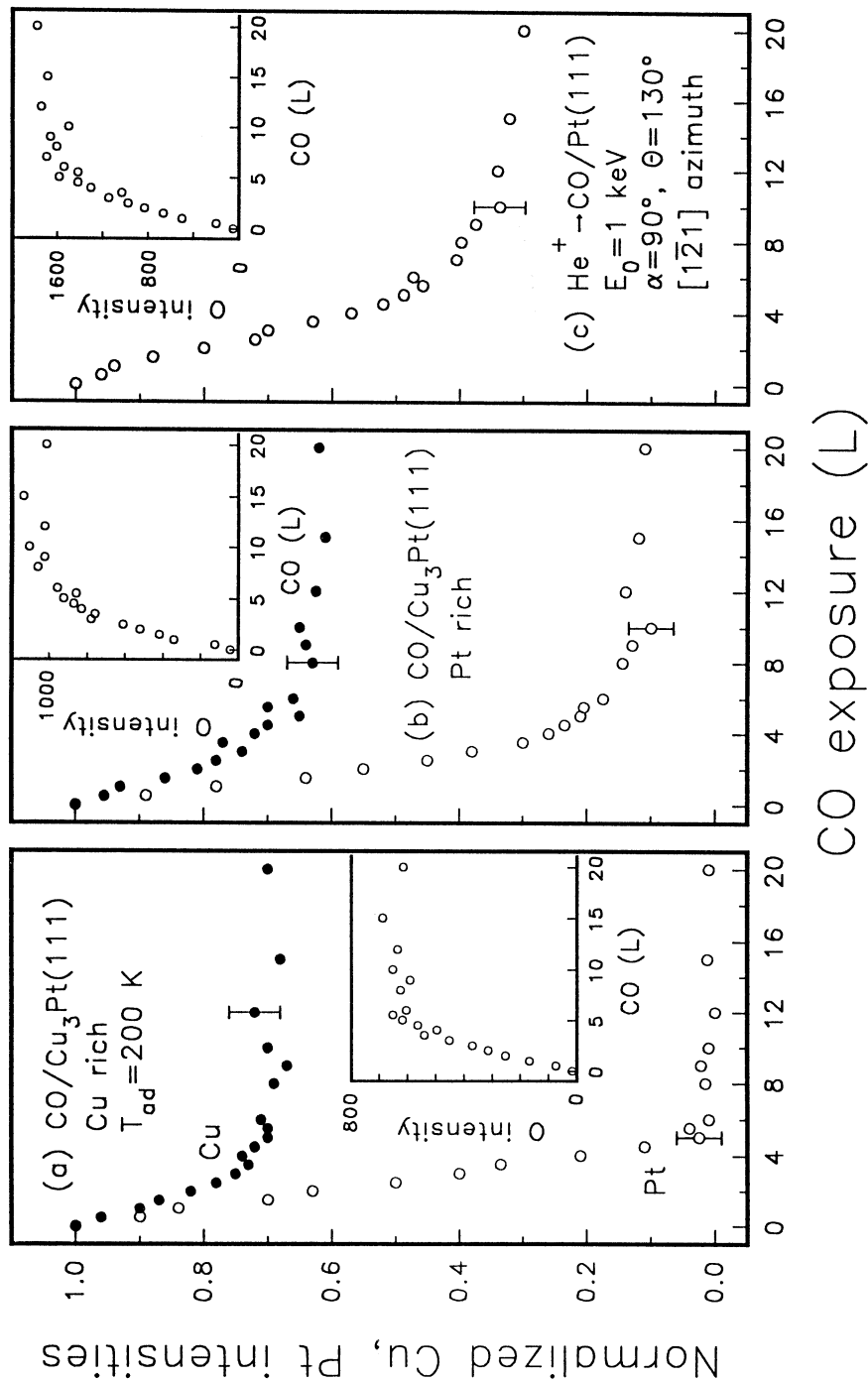


Fig. 6. Normalised Pt and Cu intensities as a function of CO exposure at a pressure of 5×10^{-8} mbar at 200 K: (a) the Cu-rich Cu₃Pt(111) surface, (b) the Pt-rich Cu₃Pt(111) surface and (c) the Pt(111) surface. The relationship between the O intensity and CO exposure is also shown in the insets.

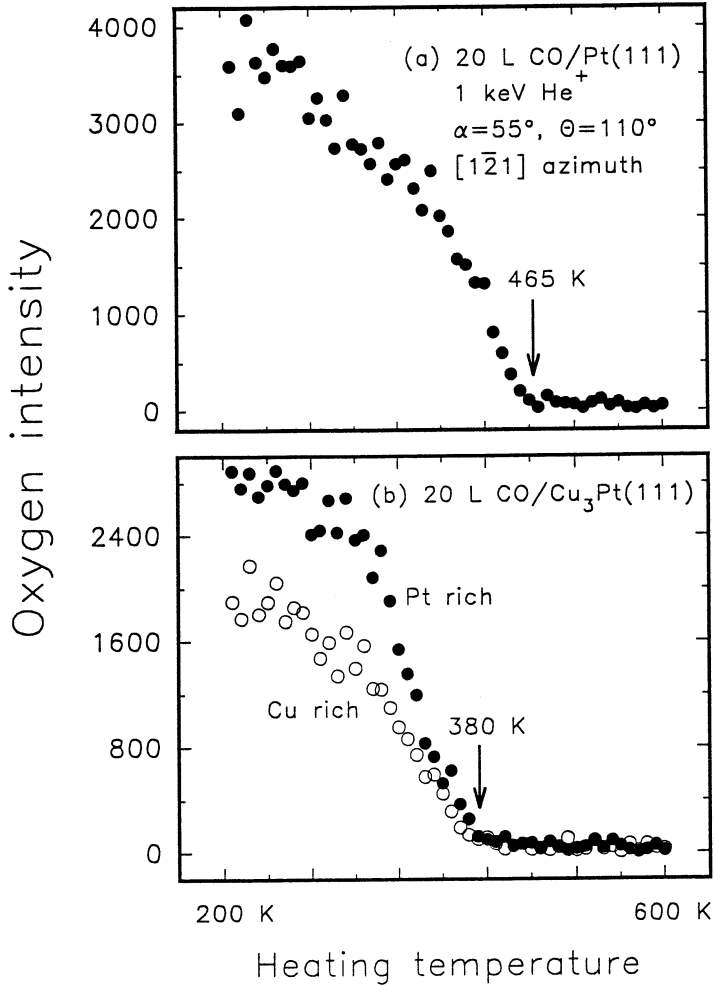


Fig. 7. The O intensities as a function of heating temperature for 1 keV He⁺ ions scattered from (a) 20 L CO/Pt(111) and (b) 20 L CO/Cu₃Pt(111) at 200 K respectively.

hybridisation band into the He ground state. Since CO adsorption causes little change in the work function of the alloy in this experimental condition, there should be no remarkable influence on the probability of the Auger transition. However, changes in ion neutralisation upon changing the electronic nature of the surface may play an important role in the relative signal intensity from the two surface constituents.

We can safely conclude that both neutralisation and shadowing are responsible for the decrease in the Cu intensity upon CO adsorption. Using CO on a Cu-rich surface as a simple case (Pt atoms are isolated by Cu atoms), in the following discussion section we propose that the shadowing of Cu along long $[1\bar{2}1]$ azimuths is due to molecular vibrations of CO closing up the narrow space between $[1\bar{2}1]$ rows. The attenuation of the Cu intensity observed along short $[0\bar{1}1]$ azimuths

is due to normal CO shadowing and/or blocking along this CO-containing row.

There is another observation of interest. In this experiment, the Pt(111) and Cu₃Pt(111) crystals were saturated with CO (~ 20 L) at 200 K, and then the energy spectra were collected as a function of heating temperature. This is shown in Fig. 7. The results indicate that the O signal is no longer detectable on the Pt(111) surface at a temperature of ~ 465 K (Fig. 7a). In contrast, the temperature for the total disappearance of the O signal on both Cu₃Pt(111) surface states is shifted by as much as ~ 85 K to a lower temperature of ~ 380 K with respect to the Pt(111) surface (Fig. 7b).

4. Discussion

The surface composition of the alloys results from the minimisation of the surface Gibbs energy. The ion scattering results in Fig. 1 confirm that the surface composition of the Cu₃Pt(111) alloy is highly influenced by surface effects. The segregation behaviour of the Cu₃Pt(111) crystal is dependent on the thermal treatment following the ion bombardment of the cleaning procedure. After stabilisation at a temperature of ~ 800 K, the crystal presents a slightly higher Cu content in the surface region. Stabilisation at lower temperature (~ 500 K) after Ar sputtering induces an Pt enrichment, leading to a value of Cu₆₈Pt₃₂ in the first layer. Such behaviour is understandable if a well known criterion (the compensation of two driving forces: surface energy and size difference) to predict which element will segregate is considered.

The bulk phase diagram (Hansen and Anderko 1958) for Cu–Pt alloys form several ordered structures at low temperatures. It seems likely that the surfaces of Cu₃Pt alloys would also be ordered. However, evidence for surface long range ordering was not observed during the whole course of the experiment. Actually, our LEED showed sharp spots with a quite low background, typical of a well-ordered lattice with a rather complete chemical disorder (see Fig. 2).

In a previous study using X-ray diffraction and thermodynamic techniques by Bidwell *et al.* (1967), rather complex ordering behaviour within the Cu₃Pt region was reported. It was found that Cu₃Pt alloys near stoichiometry exhibited long range order far above the thermodynamic critical temperatures. The reason for this kind of ordering phenomenon was found to be associated with two-stage ordering processes, which might be related to a possible periodic antiphase domain (APB) structure similar to those observed in Cu₃Pd (Bidwell *et al.* 1967). Furthermore, from the phase diagram for Cu₃Pt the stable phase of the L₁₂ structure is displaced off stoichiometry to a composition of 15 at% Pt (Hansen and Anderko 1958). Therefore, the relative phase stability of the L₁₂ structure at stoichiometry in Cu₃Pt alloy becomes lower than that in Cu–15 at% Pt alloy and as a result, the degree of long range order cannot be developed enough at stoichiometry. It was also reported by Miura *et al.* (1992) that two-stage ordering in Cu₃Pt alloys is strongly dependent on the alloy composition. As the composition deviates from 15 at% Pt in either direction, the driving force for ordering decreases. All these may explain the causes for failure to observe the LEED (2 \times 2) patterns in the present study.

For the $\Delta\phi$ values measured from both Pt(111) and Cu₃Pt(111) (Fig. 3), we found a dependence on coverage qualitatively in agreement with earlier work (Norton *et al.* 1979; Steininger *et al.* 1982; Schneider *et al.* 1994). According to

the generally accepted model for CO chemisorption, bond formation takes place mainly through coupling of the CO 5σ orbitals to the sp-band of the metal and the metal backdonates d-electrons into the CO $2\pi^*$ orbitals. With respect to the C-O bond, the 5σ orbitals are essentially non-bonding whereas the $2\pi^*$ orbitals are anti-bonding. For CO/Pt(111), the $\Delta\phi_{\min}$ at $\theta_{\text{CO}} = 0.33$ ML is reached where on-top sites are occupied only (Tüshaus *et al.* 1987; Schweizer *et al.* 1989). The $\Delta\phi$ therefore indicates charge transfer to the substrate for on-top bonded CO. At $\theta_{\text{CO}} = 0.5$ ML, the $\Delta\phi$ value is close to ~ 0.0 eV, indicating charge transfer from the substrate to the molecule for bridge bonded CO (Tüshaus *et al.* 1987; Schweizer *et al.* 1989). For CO/Cu₃Pt(111), CO adsorption induced little change of the work function. It has been reported (Schneider *et al.* 1994) that CO adsorption on Cu₃Pt(111) exhibits a vanishing dipole moment, $\mu_A \approx 0.0$ Debye. This type of adsorbate complex obviously causes only a negligible change of the work function, in reasonable agreement with the present observations.

At the adsorption temperature used in this study (200 K), pure Pt(111) has two different types of adsorption sites (on-top and bridge) for CO (Tüshaus *et al.* 1987; Schweizer *et al.* 1989). For CO on a Cu-rich Cu₃Pt(111) surface (Fig. 6a), only one site (on-top) is occupied by CO. Since the clean and annealed Cu₃Pt(111) surface is not clustered (Shen *et al.* 1995a), the CO could be able to adsorb on isolated Pt sites in a one-to-one ratio, causing the total disappearance of the surface Pt signals. However, in a Pt-rich surface (Fig. 6b) there are some Pt-Pt neighbours (Shen *et al.* 1995a), and this will result in CO bonding to Pt sites in a lower ratio depending on the Pt concentration. As the CO coverage increases, the distance between CO molecules decreases. This would result in an increase in their mutual repulsive intensity, causing CO bonds to the Pt-Cu mixed sites.

As mentioned previously, the Cu intensity during CO adsorption also decreases due to the combined effect of shadowing and neutralisation. In order to estimate the shadowing effect along long $[1\bar{2}1]$ azimuths (Fig. 6a) on a Cu-rich surface due to CO molecular vibrations, we need to know the shadowing cone radii with a combination of vibrational amplitudes of C and O atoms parallel to the surface. According to Madey (1979), the mean square vibrational amplitude of CO parallel to the surface on Ru(0001) is 0.29 Å at 300 K and 0.20 Å at 100 K, respectively. Using the reference data and Madey's method of calculation, we obtain a value of the O rms vibrational amplitude of 0.25 Å for CO on Cu₃Pt(111) at 200 K. The shadow cone radius for 1 keV He⁺ scattering off O under the experimental conditions has also been calculated. The interaction between He and O is approximated by the Thomas-Fermi-Molière (TFM) scattering potential. The parameters used in this calculation were (Ogletree *et al.* 1986): C-O bond length of 1.15 Å and C-Pt interlayer spacing of 1.85 Å, which corresponds to a value of $L_{\text{O-Pt}} = 3.0$ Å between the O and Pt atoms. The calculated curve is shown in Fig. 8, where the minimum R_0 (0.91 Å) is the shadow cone radius at the distance $L_{\text{O-Pt}}$ (3.0 Å), and s_0 (0.60 Å) is the corresponding impact parameter.

If we assume a value of 0.91 Å for the shadow cone radius of O scattered by 1 keV He⁺ ions and a horizontal vibrational amplitude of 0.25 Å for O in adsorbed CO at 200 K, then we can estimate the width of channels which exist between rows of CO adsorbed on Cu₃Pt(111) for the path of the He-Cu collisions. The row spacing along the $[1\bar{2}1]$ azimuth is 1.31 Å, and the channel is only ~ 0.2 Å wide.

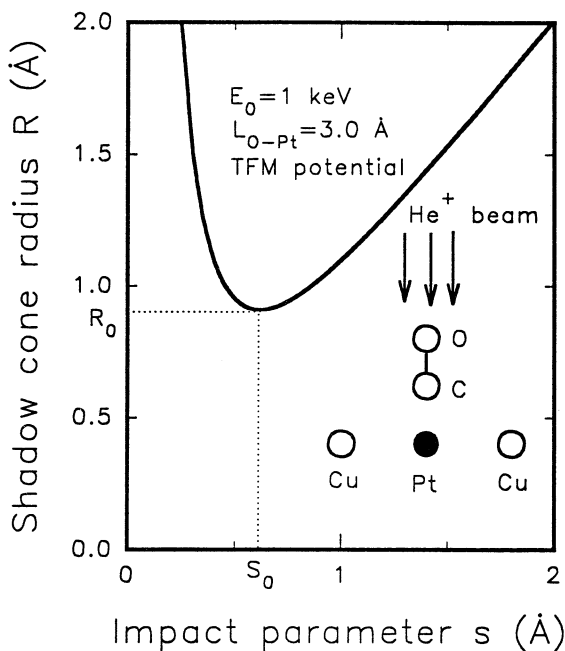


Fig. 8. Calculated shadow cone curve using the TFM potential for 1 keV He^+ ion scattering from CO/ $\text{Cu}_3\text{Pt}(111)$ at normal incidence along the $[\bar{1}\bar{2}1]$ exit azimuth.

Although these numbers are estimates, we believe that the channel in the $[\bar{1}\bar{2}1]$ azimuth may be totally perturbed and completely blocked depending on the CO coverage, i.e. the number of Pt atoms for CO occupation. The effect is believed to be the cause of the reduction in the number of particles scattered from Cu in the $[\bar{1}\bar{2}1]$ azimuth, rather than CO in the Cu sites. We have to point out here that neutralisation also contributes to the decrease in the Cu intensity on the CO-covered alloy surface, although we cannot know which process dominates during the scattering process. Due to the unknown neutralisation probability for CO adsorbed systems, the influence of the shadowing effect caused by CO vibration is difficult to assess quantitatively. More theoretical and experimental studies are needed to point the way towards a separation and a better understanding of this process.

By analysis, the decrease in the Cu intensity in short $[0\bar{1}1]$ azimuths on the Cu-rich surface (not shown) is due to the Cu atoms directly shadowed and/or blocked by the CO molecules along this CO-containing row under this geometrical condition ($\alpha = 90^\circ$ and $\theta = 130^\circ$). Since the channel in short $[0\bar{1}1]$ azimuths is sufficiently wide (2.26 Å), it is not going to be blocked by the transverse 2-D rms thermal vibration of CO relative to the interior neighbour atoms between $[0\bar{1}1]$ rows. Analysis of the shadowing effect caused by thermal vibration of CO on a Pt-rich $\text{Cu}_3\text{Pt}(111)$ surface was not attempted in this study owing to complex effects of two adsorption sites involved.

Our He^+ scattering results on CO saturated $\text{Cu}_3\text{Pt}(111)$ surface have shown a significant decrease in the temperature of the desorption with respect to the pure

Pt(111) surface (Fig. 7). If we assume that the ion beam induced sputtering effect is negligible and the CO desorption temperature is proportional to the strength of the CO–Pt bond, this shift of the CO desorption temperature is indicative of the weakened metal–CO interaction on Cu₃Pt(111). This destabilisation of the CO bonding strength on Cu₃Pt(111) is in agreement with the HREELS and UPS results, in which Schneider *et al.* (1994) found a lowering of the CO–Pt vibration frequency for the alloy surface compared with Pt(111). In addition, recent theoretical calculations by Castro and Doyen (1994) have shown that for CO/Cu₃Pt(111) the local electron structure near the Pt atoms is of predominant importance. The decrease in the energy of desorption of CO from the Pt at the Cu₃Pt(111) surface compared to a pure Pt(111) surface is due to the reduced number of Pt atoms rather than to a band structure effect (Castro and Doyen 1994).

5. Conclusion

The following general features of CO adsorption on the Cu₃Pt(111) surface have been investigated by LEIS, LEED and $\Delta\phi$ measurements.

(1) The two surface states have been evidenced depending on sputtering and annealing conditions: annealing at 850 K results in a slightly Cu-rich surface; sputtering followed by annealing at 500 K in a Pt-rich surface.

(2) CO adsorption at 200 K shows that CO bonds to the Pt sites under the experimental conditions and, moreover, that not all the Pt sites are covered by CO in a Pt-rich surface.

(3) The presence of the CO adsorbed surface layer does not induce surface segregation of Pt from the bulk. With increasing CO coverage on the Pt-rich surface, the distance between CO molecules decreases, increasing their mutual repulsive interactions and, thus, possibly the Pt–Cu mixed sites may be occupied.

(4) During CO adsorption, the decrease in the Cu intensity has been ascribed to a combined effect of neutralisation and shadowing. For CO on a Cu-rich surface, a combination of shadow cone widths and vibrational amplitudes of the O atom in CO molecules restricts the channel widths, which can explain the reduction in scattering intensity from Cu in the $[1\bar{2}1]$ azimuth without invoking CO occupation of on-top Cu sites.

Acknowledgments

The authors acknowledge stimulating discussions with Prof. Dr K. Wandelt at the University of Bonn. We are also very grateful to Prof. Dr Horst Niehus at Humboldt University, Berlin for the loan of a Pt(111) sample. This work was supported by the Australian Research Grants Scheme.

References

- Arola, E., Barnes, C. J., Rao, R. S., Bansil, A., and Pessa, M. (1991). *Surf. Sci.* **249**, 281.
- Banhart, J., Weinberger, P., and Voitländer, J. (1989). *Phys. Rev. B* **40**, 12079.
- Bidwell, L. R., Schulz, W. J., and Saxer, R. K. (1967). *ACTA Metall.* **15**, 1143.
- Castro, G. R., and Doyen, G. (1994). *Surf. Sci.* **307–309**, 384.
- Castro, G. R., Schneider, U., Busse, H., Janssens, T., and Wandelt, K. (1992). *Surf. Sci.* **269/270**, 321.
- Hagstrum, H. D. (1954). *Phys. Rev.* **96**, 336.
- Hansen, M., and Anderko, K. (1958). 'Constitution of Binary Alloys' (McGraw–Hill: New York).

- Jonstec, H. C. de, and Ponec, V. (1980). *J. Catal.* **63**, 389.
- Langeveld, A. D. van, and Ponec, V. (1983). *Surf. Sci.* **126**, 702.
- Madey, T. E. (1979). *Surf. Sci.* **79**, 575.
- Mitsui, K., Mishima, Y., and Suzuki, T. (1986). *Phil. Mag. A* **53**, 357.
- Miura, S., Mitsui, K., Tanaka, Y., Mishima, Y., and Suzuki, T. (1992). *Phil. Mag. A* **65**, 737.
- Niehus, H., Heiland, W., and Taglauer, E. (1993). *Surf. Sci. Rep.* **17**, 213.
- Norton, P. R., Goodale, J. W., and Selkirk, E. B. (1979). *Surf. Sci.* **83**, 189.
- Ogletree, D. F., Van Hove, M. A., and Somorjai, G. A. (1986). *Surf. Sci.* **173**, 351.
- Persson, B. N. J. (1992). *Surf. Sci. Rep.* **15**, 1.
- Rabalais, J. W. (1994). *Surf. Sci.* **299/300**, 219.
- Schneider, U., Castro, G. R., and Wandelt, K. (1993). *Surf. Sci.* **287/288**, 146.
- Schneider, U., Busse, H., Linke, R., Castro, G. R., and Wandelt, K. (1994). *J. Vac. Sci. Technol. A* **12**, 2069.
- Schröder, U. (1995). PhD Dissertation, University of Bonn.
- Schweizer, E., Persson, B. N. J., Tüshaus, M., Hoge, D., and Bradshaw, A. M. (1989). *Surf. Sci.* **213**, 49.
- Shek, M. L., Stefan, P. M., Lindau, I., and Spicer, W. E. (1983). *Phys. Rev. B* **27**, 7288.
- Shen, Y. G., O'Connor, D. J., and MacDonald, R. J. (1992). *Surf. Interface Anal.* **18**, 729.
- Shen, Y. G., O'Connor, D. J., Wandelt, K., and MacDonald, R. J. (1995a). *Surf. Sci.* **328**, 21.
- Shen, Y. G., Yao, J., O'Connor, D. J., Wandelt, K., and MacDonald, R. J. (1995b). *Aust. J. Phys.* **48**, 713.
- Shen, Y. G., O'Connor, D. J., Wandelt, K., van Zee, H., and MacDonald, R. J. (1995c). *Thin Solid Films* **263**, 72.
- Steininger, H., Lehwald, S., and Ibach, H. (1982). *Surf. Sci.* **123**, 264.
- Tüshaus, M., Schweizer, E., Hollins, P., and Bradshaw, A. M. (1987). *J. Electron Spectrosc. Relat. Phenom.* **44**, 305.

Manuscript received 7 July, accepted 20 September 1995